Carboxylate Binding Modes in Zinc Proteins: A Theoretical Study

Ulf Ryde
Department of Theoretical Chemistry, Chemical Centre, Lund University, S-221 00 Lund, Sweden

ABSTRACT The relative energies of different coordination modes (bidentate, monodentate, *syn*, and *anti*) of a carboxylate group bound to a zinc ion have been studied by the density functional method B3LYP with large basis sets on realistic models of the active site of several zinc proteins. In positively charged four-coordinate complexes, the mono- and bidentate coordination modes have almost the same energy (within 10 kJ/mol). However, if there are negatively charged ligands other than the carboxylate group, the monodentate binding mode is favored. In general, the energy difference between monodentate and bidentate coordination is small, 4–24 kJ/mol, and it is determined more by hydrogen-bond interactions with other ligands or second-sphere groups than by the zinc-carboxylate interaction. Similarly, the activation energy for the conversion between the two coordination modes is small, ~6 kJ/mol, indicating a very flat Zn-O potential surface. The energy difference between *syn* and *anti* binding modes of the monodentate carboxylate group is larger, 70–100 kJ/mol, but this figure again strongly depends on interactions with second-sphere molecules. Our results also indicate that the pK_a of the zinc-bound water ligand in carboxypeptidase and thermolysin is 8–9.

INTRODUCTION

The zinc peptidases are a large family of proteolytic enzymes containing a catalytic zinc ion (Lipscomb and Sträter, 1996). The two most well-known members of this group are carboxypeptidase (EC 3.4.17.1) and thermolysin (EC 3.4.24.27). Both enzymes were among the first proteins examined by x-ray crystallography, and they have been studied extensively by biochemical and structural means (Matthews, 1988; Christianson and Lipscomb, 1989; Lipscomb and Sträter, 1996).

Although the two enzymes are genetically unrelated, their active sites are almost superimposable. The catalytic zinc ion is bound to the enzymes by two histidine (His) nitrogen atoms and a glutamate (Glu) carboxylate group. In addition, an extraneous ligand, usually water, binds to the zinc ion. In carboxypeptidase, the glutamate group binds to zinc in a bidentate fashion (both Zn-O distances are 210–240 pm; Rees et al., 1983). For thermolysin, the coordination is less clear. The original report described the structure as four-coordinate with a monodentate carboxylate (Matthews et al., 1972). However, a later structure has been interpreted as five-coordinate with a bidentate carboxylate group (Holland et al., 1995). The discrepancy between the two structures has been attributed to differences in the crystallization buffer, especially the pH. Yet, some related enzymes have the same zinc ligands and a clearly monodentate carboxylate group, e.g., pseudolysin (formerly elastase, EC 3.4.24.26), with Zn-O distances of 184 and 296 pm (Thayer et al., 1991). Moreover, other proteins exhibit a coordination that is intermediate between mono- and bidentate, e.g., bacillolysin, which has Zn-O distances of 210 and 250 pm (Lipscomb and Sträter, 1996), and the sonic hedgehog protein, with Zn-O distances of 196 and 281 pm (Hall et al., 1995).

Thus these groups of zinc proteases have the same zinc ligands but exhibit different carboxylate coordination modes. The question then naturally arises, why does the coordination differ, i.e., in what way is one structure stabilized in some proteins but another in other proteins? Such a question also has a strong bearing on other proteins. Carboxylate ligands are common ligands in many zinc as well as iron and calcium proteins. For example, all mono- and binuclear nonheme iron proteins and all polynuclear zinc proteins have at least one carboxylate group per metal ion (Holm et al., 1996; Lipscomb and Sträter, 1996). Moreover, it is well known that these carboxylate groups often shift between mono- and bidentate coordination and between binding to one or two metal ions. This flexible motion is believed to be of catalytic significance and has been termed *carboxylate shift* (Lippard and Berg, 1994).

In this paper we study the energetics of various coordination modes of a carboxylate group in a number of realistic model systems using advanced quantum chemical methods. We have chosen to start with zinc systems, because Zn^{2+} is a closed-shell ion that gives more accurate results in quantum chemical calculations than open-shell iron ions, and because we can directly relate the results to the relative simple zinc peptidases. The investigation includes not only mono- and bidentate coordination, but also *syn* and *anti* coordination modes of the carboxylate group.

Received for publication 2 February 1999 and in final form 10 June 1999.
Address reprint requests to Dr. Ulf Ryde, Department of Theoretical Chemistry, Chemical Centre, Lund University, P.O.B. 124, S-221 00 Lund, Sweden. Tel.: 46-46-222 45 02; Fax: 46-46-222 45 43; E-mail: ulf.ryde@teokem.lu.se.

0006-3495/99/11/2777/11 $2.00

METHODS

The zinc ligands histidine and glutamate (or aspartate) were modeled by imidazole (Im) and acetate (Ace), respectively. Initial calibrations have shown that this is the smallest model for which reliable data are obtained; if the carboxy-

late ligand is instead modeled by a formate ion, the distances to Zn may change by up to 4 pm and relative energies by ~4 kJ/mol, and if ammonia is used as a model of histidine, qualitatively erroneous structures may be obtained because of hydrogen-bond interactions with the polar hydrogens on ammonia. Because the potential surfaces of the models are very flat, tight convergence thresholds were used in the geometry optimizations: 10^{-7} Hartree for the change in energy between two iterations (0.26 J/mol) and 10^{-4} a.u. for the norm of the internal gradients (0.0053 pm or 0.0057°). The full geometry of all models was optimized, and several starting structures were tested to reduce the risk of being trapped in local minima. Only the structures with the lowest energy are reported. Symmetry (at most C_s) was used in the calculations only if initial geometry optimizations based on asymmetrical structures indicated that the complex actually is symmetrical.

The geometry optimizations were performed with the hybrid density functional method B3LYP (restricted formalism) as implemented in the Turbomole software (Ahlrichs et al., 1989). This method differs slightly from the one defined in the Gaussian quantum chemistry software (Frisch et al., 1998) in that it uses the Ceperley-Alder solution to the uniform electron gas in the Vosko-Wilk-Nusair correlation functional (keyword VNW5 in the Gaussian 98 manual; Hertwig and Koch, 1997); this is the fit recommended by the authors (Vosko et al., 1980).

The B3LYP method has been shown to be the most accurate density functional method (Bauschlicher, 1995), and it gives as good or better geometries and energies as correlated ab initio methods for first-row transition metal complexes (Ricca and Bauschlicher, 1995; Holthausen et al., 1995). However, few investigations have been performed on zinc complexes. Therefore we first compared geometries obtained by the B3LYP method with those obtained by the restricted Hartree-Fock method (RHF) and with second-order Møller-Plesset perturbation theory (MP2) for some small model complexes. The semiempirical AM1 and PM3 methods were also tested but turned out to give highly unreliable results. The results in Table 1 show that the B3LYP geometries are almost identical to the MP2 geometries and much better than Hartree-Fock geometries. Thus the distances to and the bond angles around the zinc ion change by less than 1 pm and 2°, respectively, when the method is changed from MP2 to B3LYP. Consequently, B3LYP also seems to perform excellently for zinc complexes and was therefore used in the rest of this investigation.

After an extensive calibration procedure, we decided to use in the geometry optimizations the double-ζ zinc basis (62111111/33111/311) of Schäfer et al. (1992), enhanced with *p*, *d*, and *f* functions with exponents 0.162, 0.132, and 0.39 (called DZpdf) and the polarized split-valence Dunning-Hay (1977) basis set for the other atoms, without polarization functions on hydrogen but with diffuse functions on the O atoms. Only the pure 5*d* and 7*f* type functions were used. Diffuse functions on the O atoms are necessary to get accurate Zn-O distances (especially for water). However, diffuse functions are not necessary on N and C atoms; their inclusion leads to changes in the geometry and relative energies by less than 0.8 pm and 0.3 kJ/mol.

When the optimal geometries were found, single-point energy calculations were performed with the B3LYP method using a larger basis set: for Zn we used the DZpdf basis set, enhanced with *s*, *p*, and *f* functions with exponents 0.012237, 0.047769, and 3.89, respectively, whereas the 6–311+G(2d, 2p) basis set (Here et al., 1986) was used for the other atoms. Thermodynamic corrections were added to all energies, i.e., the translational, rotational, and vibrational (including zero-point energy) contributions to Gibbs free energy at 300 K and 101.3 kPa pressure. These were calculated from the vibrational frequencies, obtained with the same basis sets as in the geometry optimizations using the Gaussian-98 program (Frisch et al., 1998), and they were uniformly scaled by a factor of 0.963 (Rauhut and Pulay, 1995). All other calculations were performed with the Turbomole 2.1 software (Ahlrichs et al., 1989) on SGI R10000 workstations. Force constants for the Zn-ligand bonds where calculated from the vibrational frequencies, using the

TABLE 1 Performance of the B3LYP method

		Distance to Zn (pm)					Angle around Zn (°)				
Complex	Method	N1	N2	O_1	O_2	O_3	N—N	N—O_1	N—O_3	O_1—O_2	O_1—O_3
A	RHF	208.6	208.6	202.4	202.9		119.5	115.2		64.6	
A	MP2	205.3	205.3	204.2	204.2		120.5	114.5		66.1	
A	B3LYP	205.0	205.0	203.5	203.6		120.3	114.7		65.8	
A(H_2O)	RHF	211.2	211.2	203.6	213.8	217.7	117.2	97–120	100.4	62.4	82–145
A(H_2O)	MP2	207.3	207.2	204.9	216.4	216.6	119.6	97–119	101.0	63.7	80–144
A(H_2O)	B3LYP	207.1	207.1	204.7	215.5	216.7	119.1	97–120	100.3	63.5	81–144
A(OH^-)	RHF	215.2	219.8	195.2	322.8	185.7	108.5	104.1	92–114	43.6	130.7
A(OH^-)	MP2	210.6	215.5	196.6	324.1	186.5	110.8	104.0	88–118	44.3	129.4
A(OH^-)	B3LYP	209.8	215.9	196.4	325.0	186.0	111.4	103.5	87–120	43.8	128.6

Geometries are compared for three small model systems calculated with three different methods (B3LYP, RHF, and MP2). No symmetry restrictions were imposed. O_1, O_2, and O_3 are the two oxygen atoms of the carboxylate group and the oxygen of water or the hydroxide ion, respectively. A = $Zn(NH_3)_2(HCOO)^+$. The basis sets used were slightly smaller than the standard ones: no extra *d* and *f* functions on Zn and no diffuse functions on O.

method suggested by Seminario (1996), which is invariant with the choice of internal coordinates.

RESULTS AND DISCUSSION

Carboxypeptidase and thermolysin models with water

The active-site zinc ion in carboxypeptidase and thermolysin is bound by two histidine residues and a glutamine carboxylate group. In addition, an exogenous ligand binds to the zinc ion, and it may be a substrate, an inhibitor, water, or a hydroxide ion. It turned out that the energetics of the carboxylate binding depend quite strongly on this exogenous ligand, so we investigated two typical cases, viz. binding of water or a hydroxide ion.

When the exogenous zinc ligand is a water molecule, the most stable coordination mode of the carboxylate group is monodentate. As can be seen in Fig. 1, the monodentate structure of $Zn(Im)_2(Ace)(H_2O)^+$ is distinctly asymmetrical, with the two imidazole rings tilted with respect to each other and with one of the water hydrogens out of the carboxylate-zinc plane. The structure is stabilized by a very strong hydrogen bond between the noncoordinating carboxylate oxygen and the in-plane water hydrogen (145 pm). In addition, there are two weak C-H···O hydrogen bonds between the imidazole rings and the zinc-bond carboxylate and water oxygen atoms, respectively (268–279 pm), explaining the differing orientation of the imidazole rings. The Zn-O distances are 195 and 312 pm for the carboxylate group and 203 pm for water. The Zn-O-C angle is 121°, close to an ideal sp^2 angle. Further interesting geometric parameters are listed in Table 2.

There is also a local minimum of $Zn(Im)_2(Ace)(H_2O)^+$, with the carboxylate group coordinating to zinc by its both oxygen atoms. It is only 10 kJ/mol less stable than the monodentate structure. As can be seen in Fig. 2, the structure is moderately asymmetrical (one of the water hydrogens is out of the carboxylate-zinc plane, but the imidazole rings are nearly symmetrical). The lower stability of this structure is due to the much weaker hydrogen bond between water and the carboxylate group (234 pm, with a O-H-O angle of 108°). This is only partly compensated for by three week C-H···O hydrogen bonds between imidazole and the carboxylate and water oxygens (257–288 pm). The two carboxylate oxygens are 205–216 pm from the zinc ion, leading to an increased Zn-O distance for water (223 pm). The two Zn-O-C angles are 87° and 92°.

To get an estimate of the barrier between the monodentate and bidentate structures, we also optimized the transition state between them. As can be seen in Fig. 3, it is rather similar to the bidentate complex. The carboxylate Zn-O distances are 199 and 237 pm, whereas the distance to the water molecule is 214 pm. There is a fairly strong hydrogen bond between the water molecule and the carboxylate oxygen with the longer bond (197 pm), and there are two hydrogen bonds between the imidazole rings and the other carboxylate oxygen and the water oxygen (262–278 pm). Interestingly, the transition state is only 6 kJ/mol less stable than the bidentate structure (15 kJ/mol less stable than the monodentate structure). Thus the carboxylate shift reaction in this system is almost barrierless, and the energy difference between the two states is small.

In the monodentate structure (Fig. 1), there is a hydrogen bond between the nonligating carboxylate atom and the zinc-bound water molecule, and the water oxygen is within the carboxylate-zinc plane. This is the first of two typical interactions between a metal-bound carboxylate and a water molecule observed in protein structures (Chakrabarti, 1990). The other interaction (called type 2), which is almost twice as common, involves a bidentate carboxylate group, where the zinc-water bond is perpendicular to the carboxylate-zinc plane. This is the structure encountered in carboxypeptidase, but it is not the bidentate structure optimized by us. In

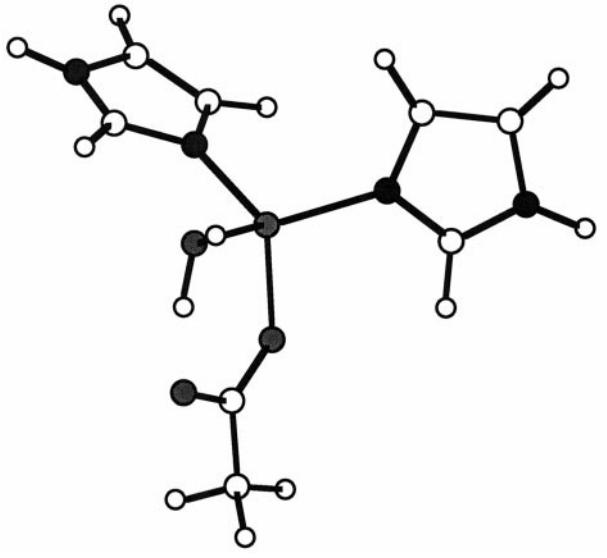

FIGURE 1 The optimized monodentate structure of $Zn(Im)_2(Ace)(H_2O)^+$.

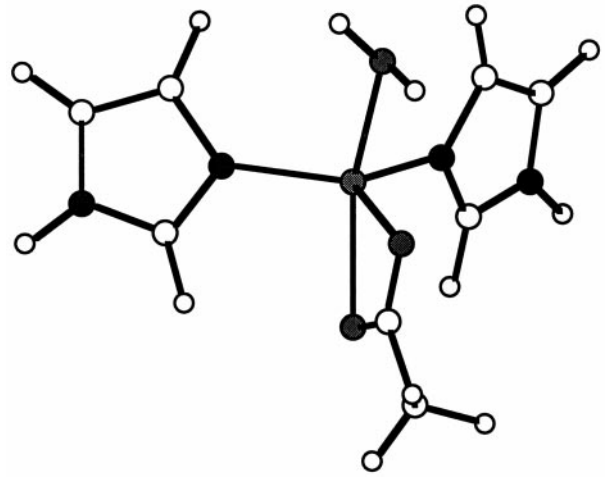

FIGURE 2 The optimized bidentate structure of $Zn(Im)_2(Ace)(H_2O)^+$.

TABLE 2 Geometric parameters and relative energies of the optimized complexes and a number of protein crystal structures

Complex	Coord mode	Relative energy	Distance to Zn (pm)					
			N_1	N_2	O_1	O_2	O_3	O_4
$Zn(Ace)^+$	Bi	0.0			196	196		
	Mon*	89.4			181	294		
	Anti	131.0			196	196		
$Zn(Im)_2(Ace)^+$	Bi	0.0	199	199	204	205		
	Mon*	45.7	198	198	186	294		
	Anti	95.3	197	197	183	406		
$Zn(Im)_2(Ace)(H_2O)^+$	Mon	0.0	201	201	194	310	203	
	Bi	9.7	201	202	205	216	223	
	Bi, T2	24.0	205	205	213	213	215	
	TS[#]	15.4	201	204	199	237	214	
	Anti	87.1	199	201	188	409	216	
$Zn(Im)_2(Ace)(H_2O)^+ + (H_2O)$	Mon	15.7	200	202	196	312	203	
	Bi	0.0	202	203	205	230	212	
	Bi, T2	2.2	203	204	206	225	211	
$Zn(Im)_2(Ace)(H_2O)^+ + (H_2O)_2$	Mon	9.6	201	203	196	307	202	
	Bi	0.0	202	203	203	235	213	
	Bi, T2	1.2	203	203	206	230	212	
Carboxypeptidase (5cpa)			207	213	218	231	205	
Thermolysin (1lnf)			198	199	224	238	228/238[‖]	
Thermolysin (8tln)			193	197	188	279	216	
Pseudolysin (1eza)			205	209	184	296	236	
$Zn(Im)_2(Ace)(OH)$	Mon	0.0	209	209	196	304	188	
	Bi[§]	22.3	212	212	215	222	191	
	Anti	68.3	212	212	190	413	189	
$Zn(Im)_2(Ace)_2$	Mon	0.0	205	208	196	330	195	289
	Bi[¶]	11.1	207	212	195**	287**	201**	241**
	Bi[¶]	6.3	206	208	199	339	200	241**
	Bi[¶]	3.4	207	209	196	287**	195	297
	Bi[§]	12.9	212	212	195	304	218	220
	Bi[§]	13.9	206	210	212	221	196	330
Carboxypeptidase (1cbx)			204	200	203	275	230	261
Thermolysin (1 tmn)			195	204	195	287	201	241
(Im)(Ace)Zn(OH)(Ace)Zn(Im)(Ace)	Bi		205		200	264	201	199
			205		196	258	204	196
Aminopeptidase (1 amp)			232		204	238	205	225
			221		205	234	201	229
$Zn(Im)_3(Ace)^+$	1.5	0.0	204	204	199	248	208	
	Bi[§]	4.2	206	206	212	217	210	
	Mon*	4.2	204	204	193	301	204	
Fuculose 1-phosphate aldolase (1 fua)			199	207	189	238	209	
Adenosine deaminase (1a4m)			252	250	234	371	254	214

*This monodentate structure was obtained by constraining the Zn—O—C angle to 120°.

[#]The transition state between the mono- and bidentate structures.

[§]This bidentate structure was obtained by constraining the Zn—O—C angle to 90°.

[¶]This structure has been obtained by constraining a Zn—O distance (as indicated in the table).

[‖]The structure is disordered.

**This distance has been constrained.

The protein structures are identified by their Brookhaven protein data bank code.

[Rees et al. (1983), Holland et al. (1995), Holland et al. (1992), Thayer et al. (1991), Dreyer and Schulz (1996), Wang and Quiocho (1998), Mangani et al. (1992), Monzingo and Matthews (1984), and Chevrier et al. (1994)]. N_1 and N_2 are the coordinating nitrogens of the two (closest) imidazole groups. O_1 and O_2 are two oxygens of the (first) acetate group. In $Zn(Im)_2(Ace)(H_2O)^+$ and $Zn(Im)_2(Ace)(OH)$, O_3 is the oxygen in water or hydroxide, respectively, in $Zn(Im)_3(Ace)^+$, O_3 is the nitrogen of the most distant imidazole ligand, and in $Zn(Im)_2(Ace)_2$, O_3 and O_4 are the two oxygens in the second acetate group. Finally, in the aminopeptidase model (Im)(Ace)Zn(OH)(Ace)Zn(Im)(Ace), the ligands of each zinc ion are given on separate lines, and O_3 and O_4 are the oxygen atoms of the bridging acetate and hydroxide ions, respectively.

our bidentate structure (Fig. 2), the water molecule is in the zinc-carboxylate plane, and it forms a hydrogen bond to one carboxylate oxygen atom. We have also optimized a type 2 structure of the $Zn(Im)_2(Ace)(H_2O)^+$ complex. As can be seen in Fig. 4, this structure is symmetrical, with almost no interaction between the water molecule and the carboxylate group (the H-O distances are 320 pm). Instead, the carboxylate group forms weak hydrogen bonds with the imidazole ring (234 pm). Therefore, this structure is 14 kJ/mol less stable that the bidentate structure in Fig. 2.

The reason why the calculated relative stability of the mono- and bidentate structures, as well as the one of the two

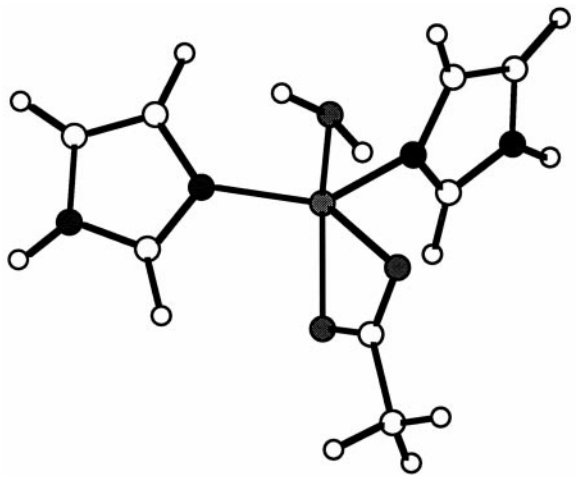

FIGURE 3 The optimized structure of the transition state between the bidentate and monodentate coordination of $Zn(Im)_2(Ace)(H_2O)^+$.

types of bidentate structures, do not reproduce the trends observed in crystal structures is most likely that the coordination mode of the carboxylate group is determined more by hydrogen-bond interactions with the surrounding protein than by the zinc-carboxylate interaction. Already in the $Zn(Im)_2(Ace)(H_2O)^+$ complexes, the coordination mode is mostly determined by hydrogen-bond interactions between the carboxylate group and the water and imidazole molecules. In a protein, many more interactions are possible, and there are smaller restrictions in the geometries attainable than in our small complexes (especially for noncoordinating water molecules). All crystal structures of zinc peptidases show several hydrogen bonds between the zinc-bound water molecule or carboxyl group and other protein residues or crystal water molecules, whereas hydrogen bonds between the various zinc ligands are rather rare. For instance, in carboxypeptidase, there are two hydrogen bonds from crystal water molecules to the carboxylate group and one hydrogen bond from the zinc-bound water molecule to a second-sphere carboxylate group (Glu^{270}), thereby stabilizing the type 2 coordination. Similarly, the monodentate crystal structures of thermolysin and pseudolysin show hydrogen bonds between both carboxylate oxygens and a water molecule (the unligated atom) or a tyrosine hydroxyl group (the ligated atom), and they have several polar interactions between the zinc-bound water molecule and various protein residues or water molecules (Holland et al., 1992; Thayer et al., 1991). Because such interactions are not included in our model systems, we cannot expect to reproduce fully the experimental trends.

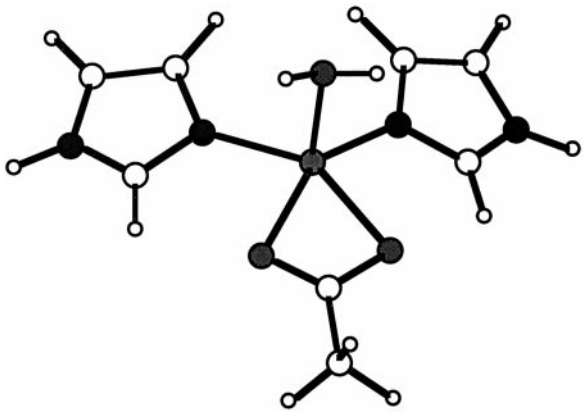

FIGURE 4 The optimized bidentate type 2 structure of $Zn(Im)_2(Ace)(H_2O)^+$.

To test the influence of second-sphere ligands on the relative energies of the studied complexes, we have optimized the structure of the monodentate and the two bidentate conformations of $Zn(Im)_2(Ace)(H_2O)$ with one or two additional water molecules in the second coordination sphere. As can be seen from the results in Table 2, the carboxylate Zn–O distances of the bidentate complexes become less similar (~205 and 230 pm, respectively), but otherwise the general structure of the complexes is not changed very much. However, the relative energies are strongly affected. The bidentate complexes form more favorable hydrogen bonds to the carboxylate group (184–192 pm) and the zinc-bound water molecule (165–171 pm) than the monodentate complex (183–230 pm), for which the carboxylate group is already involved in a hydrogen bond to the zinc-bound water. Therefore, the order of the bidentate and monodentate complexes is reversed and the bidentate complexes become most stable by ~10 kJ/mol. Moreover, the two forms of the bidentate complex have almost the same energy (within 2 kJ/mol). Thus this simple model of possible second-sphere interactions confirms our suggestion that second-sphere coordination is important for the energetics of these complexes, and they give a considerably improved correspondence to experiments. Moreover, even with second-sphere ligands, the energy differences between the various coordination modes are small, indicating that the potential surfaces are still very flat.

Carboxypeptidase and thermolysin models with a hydroxide ion

In the most widely accepted reaction mechanism of the zinc peptidases, a zinc-bound hydroxide ion is the nucleophile that attacks the peptide carbonyl atom (Lipscomb and Sträter, 1996). Thus the main function of the zinc ion is to lower the acid constant of a water molecule to physiological pH. To examine the effect of such a deprotonation on the carboxylate coordination, we also studied models involving a hydroxide ion.

The most stable configuration of $Zn(Im)_2(Ace)(OH)$ is also monodentate. As can be seen in Fig. 5, it is symmetrical and is stabilized by two hydrogen bonds between imidazole and the noncoordinating carboxylate oxygen (231 pm) and by two weaker hydrogen bonds from imidazole to the hydroxide ion (278 pm). Quite surprisingly, this conformation is more stable than one with an interaction between the

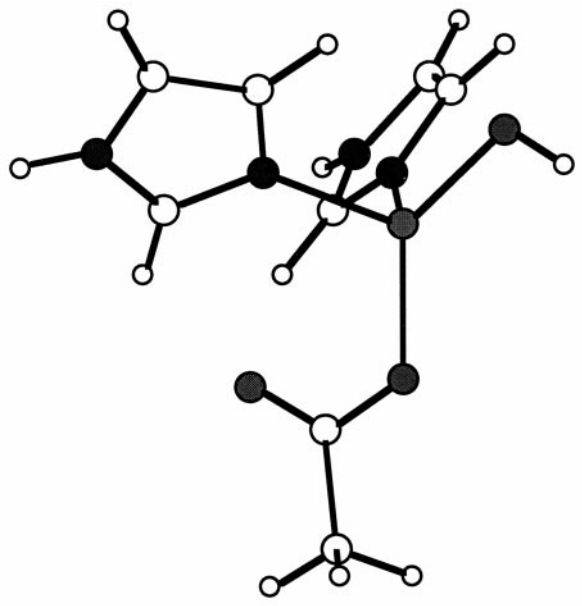

FIGURE 5 The optimized monodentate structure of $Zn(Im)_2(Ace)(OH)$.

hydroxide hydrogen and the carboxylate group (such a structure is not even a local minimum, but reorganizes to the structure in Fig. 5); evidently the hydroxide ion is too poor a hydrogen-bond donor for such an interaction. The Zn-OH bond is very short, 187 pm, and therefore the bonds to the other ligands are longer than in the corresponding water model.

We have also tried to optimize a bidentate structure of this complex. However, there does not seem to be a bidentate local minimum in the hydroxide complex. Fig. 6 shows the energy and the zinc bond lengths of the $Zn(Im)_2(Ace)(OH)$ complex as a function of the carboxylate Zn-O distance. Clearly, the curve shows no sign of a second local minimum. Still, the energies involved are rather small. At Zn-O distances typical for a bidentate complex (e.g., 213 and 220 pm), the constrained structure is only 22 kJ/mol less stable than the optimal monodentate structure. This energy difference can easily be bypassed by appropriate hydrogen bond interactions, because a hydrogen bond between water and a carboxylate or hydroxide group typically gives 70–100 kJ/mol.

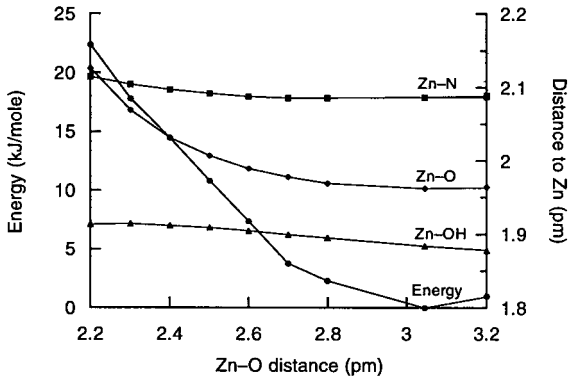

FIGURE 6 The energy of the $Zn(imidazole)_2(CH_3COO)(OH)$ complex as a function of one Zn-O bond length. All other geometric parameters were optimized at each point.

The protonation status of the extraneous zinc ligand

In Table 2, four crystal structures of zinc proteases are also included, namely those of carboxypeptidase (bidentate), pseudolysin (monodentate), and two structures of thermolysin, one bidentate and one monodentate (Rees et al., 1983; Thayer et al., 1991; Holland et al., 1992, 1995). Most of the Zn-ligand distances in these structures are quite similar to those of our optimized complexes, confirming that our methods provide reliable results. For example, the experimentally observed Zn-N distances are 193–213 pm (average 203 pm), which compare favorably with the optimized distances, 201–202 pm for $Zn(Im)_2(Ace)(H_2O)^+$ and 209–212 pm for $Zn(Im)_2(Ace)(OH)$. Similarly, our optimized distances are very close to the average distances found for zinc complexes in the Cambridge Structural Database (Alberts et al., 1998). For example, they find for four-coordinate complexes Zn-N = 201 pm, Zn-O (water or hydroxide) = 201 pm, and Zn-O (carboxylate) = 197 pm, which is very close to the optimized values of the monodentate $Zn(Im)_2(Ace)(H_2O)^+$ complex: 201, 203, 194 pm, respectively.

However, our optimized distances of the carboxylate groups are more extreme than those in the crystal structures, i.e., the optimized bidentate structures have more similar distances (205–216 pm) and the monodentate structures have more dissimilar distances (194/310 and 196/304 pm) than the crystal structures (201 $\pm$ 11 pm for monodentate structures and 216 $\pm$ 10 and 240 $\pm$ 14 pm for bidentate structures in zinc-carboxylate proteins, and 208 $\pm$ 6 and 231 $\pm$ 9 pm for bidentate zinc-carboxylate complex in the Cambridge crystal database (Alberts et al., 1998)). This is most likely due to the uncertainty in the crystal structures, combined with the fact that the optimization procedure ignores the dynamics of the very flat Zn-O potential (the optimized structures apply to a temperature of 0 K, whereas the measurements are performed at higher temperatures). It is well known that the dynamics at ambient temperatures may change the metal-ligand bond length significantly (by more than 10 pm) if the corresponding potential surface is flat (De Kerpel and Ryde, 1999). Moreover, it is clear that if a system is characterized by two local minima, which have almost the same energy and are separated by a low barrier, then both minima will be populated at room temperature and the observed bond lengths will be a Boltzmann-weighted average of the bond lengths of the two minima.

X-ray absorption fine structure (XAFS) measurements on carboxypeptidase have indicated that the active site consists of four N/O ligands at a distance of 201 $\pm$ 1 pm from the zinc ion and one O ligand at a distance of 257 $\pm$ 4 pm (in

solution; in the crystal, the values are 203 ± 1 and 236 ± 4 pm) (Zhang et al., 1992). They also estimate that the variation in the individual values of the four close ligands can be ~10–15 pm. Thus the XAFS data also indicate that the carboxylate coordination is somewhere between strictly bidentate and monodentate. Again, this is an effect of the dynamics of this system, which gives large differences between the measured and optimized distances due to the shallow Zn-O potential. If we constrain the second carboxylate Zn-O distance to 257 pm in the $Zn(Im)_2(Ace)(H_2O)^+$ complex, we get for the following optimized Zn-ligand distances: 201 pm to imidazole, 195 pm to the carboxylate oxygen, and 216 pm to water, giving an average of 203 pm, only 2 pm from the measured value. The hydroxide complex gives a similar average (202 pm), but a larger variation in the individual values (209, 199, and 190 pm). Thus our calculations give reliable structures, but (naturally) they ignore the thermal dynamics of the system.

The kinetic constants of thermolysin and carboxypeptidase exhibit two characteristic pK_a values, one around 5–6 and the other around 8–9 (Lipscomb and Sträter, 1996). There has been much debate on the assignment of these values, and no consensus seems to have been reached yet, apart from the agreement that one of the values should be assigned to the zinc-bound water (Lipscomb and Sträter, 1996). Because our calculations give reliable estimates of the Zn-ligand distances, it should be possible to determine the protonation status of the extraneous zinc ligand by comparing our optimized distances with those found in crystal structures.

First of all, we note that the $Zn\text{-}OH^-$ distance is very stable and insensitive to the coordination mode of the carboxylate group (188–191 pm; cf. Fig. 6). On the other hand, the $Zn\text{-}OH_2$ bond depends quite strongly on the coordination mode of the carboxylate ligand (and on the theoretical method) with a variation between 203 and 223 pm (cf. Table 2). This is because the force constant is much larger for the $Zn\text{-}OH^-$ bond than for $Zn\text{-}OH_2$ (60 compared to 9–20 $J/mol/pm^2$). Thus we can conclude that a $Zn\text{-}OH^-$ distance is expected to be close to 190 pm, with only a minor elongation due to dynamic effects at ambient temperatures, whereas the $Zn\text{-}OH_2$ bond can be expected to be anywhere between 200 and at least 230 pm.

The Zn-O distance for the extraneous ligand in the four crystal structures in Table 2 varies between 205 and 238 pm (average 225 pm). Thus this strongly indicates that these complexes involve a zinc-bound water molecule rather than a hydroxide ion. In fact, if the uncertainty in the Zn-O distances is ~20 pm, as is typical for structures of this resolution (Lipscomb and Sträter, 1996), only one of the structures (5cpa) is consistent with a zinc-bound hydroxide ion, and that structure is equally consistent with the optimized water structure. Thus our calculations strongly indicate that the zinc-bound water molecule is responsible for the higher pK_a. Considering that all crystal structures in Table 2 were collected at pH 7–8, i.e., between the two observed pK_a values, it seems most likely that the extraneous ligand is responsible for the higher pK_a. This is in accord with the observation that the Zn-water distance decreases with pH in a series of crystal structures of carboxypeptidase measured at pH 7.5–9 (Shoham et al., 1984).

The fact that the crystal structures are determined quite close to the pK_a of the extraneous ligand indicates that the reported structures actually are a mixture of the water and hydroxide complexes. This may explain some of the disorder seen in many of the crystal structures (Holland et al., 1995). Moreover, it will make the interpretation of the coordination mode of the carboxylate ligand harder, because our results indicate that the bidentate water complex is more stable than the bidentate hydroxide complex. Interestingly, the difference between the monodentate and bidentate crystal structures of thermolysin has been attributed to differences in the pH of the crystallization buffer, viz. that the monodentate structure was studied at a higher pH than the bidentate structure (Holland et al., 1992, 1995). This is in perfect agreement with our results.

Other proteins

Our results indicate that the relative stabilities of the mono- and bidentate coordination modes of a carboxylate group depend strongly on the other first- and second-sphere ligands. In particular, the total charge of the complex seems to be important. If it is +1, the two coordination modes have almost the same energy (and are both local minima). However, if the charge is zero or negative, the bidentate structure is destabilized and the corresponding minimum disappears in our model complexes.

This interpretation is in accord with most crystal structures of zinc proteins. For example, none of the mononuclear zinc structures with a bidentate carboxylate ligand presented in the review by Lipscomb and Sträter (1996) has a total charge of less than +1. Similarly, most bi- and trinuclear zinc sites also have monodentate carboxylates. However, there are some inhibitor complexes of carboxypeptidase and thermolysin, where a carboxyl or phosphate group of the inhibitors coordinates to the zinc ion, and either the inhibitor or the glutamine carboxylate groups (or both) show a bidentate coordination (Christianson, 1991). Yet these complexes show a clear tendency toward an elongation of one the carboxylate Zn-O bonds (225–286 pm, Christianson, 1991). Moreover, in all cases, the carboxylate or phosphate group of the inhibitor forms a short hydrogen bond (200–280 pm O-O distance) to a second-sphere glutamate residue (Glu^{270} or Glu^{143}), showing that either the glutamate residue or the inhibitor group is protonated and therefore is not negatively charged. Even if the proton is on the glutamate residue, this close interaction compensates for much of the charge on the inhibitor, which probably explains why the zinc complex may keep a bidentate coordination.

To get a more detailed picture of such complexes, we have optimized the structure of $Zn(Im)_2(Ace)_2$ as a model of

carboxypeptidase or thermolysin with a carboxylate inhibitor, e.g., L-benzylsuccinate or *N*-(1-carboxy-3-phenylpropyl)-Leu-Trp (Mangani et al., 1992; Monzingo and Matthews, 1984). The crystal structures of these protein-inhibitor complexes have carboxylate bonds that are intermediate between monodentate and bidentate (there are two short Zn-O bonds, 195–230 pm, and two longer bonds, 241–287 pm). However, for our optimized model, the coordination is different. As can be seen in Fig. 7, the optimal structure has one clearly monodentate carboxylate group (Zn-O distances 196 and 330 pm), and one group of an intermediate type (Zn-O distances 195 and 291 pm). The latter distance is quite similar to one of the crystal Zn-O distances, but the distances to the other group clearly differ. The optimized structure is stabilized by four hydrogen bonds between imidazole and the carboxylate groups, two to the noncoordinating atom at a Zn-O distance of 291 pm (232–233 pm), and one to each of the two oxygen atoms of the other carboxylate group (262 pm to the coordination atom, and 203 pm to the other).

We have tried to optimize strictly bidentate structures of either of the two carboxylate groups, but unsuccessfully. Therefore, we must conclude that the bidentate binding of one of the carboxylate groups in the proteins is stabilized by hydrogen-bond interactions with second-sphere atoms or by the reduced charge of the inhibitor discussed above. However, it should be noted that the energy difference between the optimal structure and a structure with the same carboxylate distances as in the crystal structure is only 11 kJ/mol. Thus we again see that the potential surface of the carboxylate Zn-O bonds is very flat and that the coordination geometry is determined more by interactions with outer-sphere atoms than by the Zn-O interaction. Similarly, it costs only 13–14 kJ/mol to force one of the carboxylate groups to be strictly bidentate. This is 8 kJ/mol lower than for the Zn(Im)(Ace)(OH) complex and only 4 kJ/mol more than for the $Zn(Im)(Ace)(H_2O)^+$ complex. Thus it is easier to stabilize a bidentate structure of a neutral complex if the other charged ligand is a carboxylate group than if it is a hydroxide ion.

Even if there are no unambiguous mononuclear neutral zinc complexes with a bidentate carboxylate coordination, among the bi- or trinuclear zinc proteins, there are neutral sites with a clear bidentate carboxylate ligation. One example is alkaline phosphatase (Lipscomb and Sträter, 1996), but the clearest example is aminopeptidase (Chevrier et al., 1994). The latter protein has a binuclear zinc site, where each zinc ion has one histidine ligand and one bidentate glutamate or aspartate ligand. In addition, there are two bridging molecules, an aspartate carboxylate group, and a hydroxide ion. The two bidentate carboxylate groups have quite similar Zn-O distances: 204/238 and 205/234 pm (cf. Table 2).

We have optimized the structure of (Im)(Ace)Zn(Ace)-(OH)Zn(Im)(Ace) as a model of aminopeptidase. Quite satisfactorily, the optimized structure of this complex turned out to be quite similar to the crystal structure of the protein. As can be seen in Table 2 and Fig. 8, the two zinc ions have very similar coordinations, with one bidentate carboxylate ligand on each zinc ion. The Zn-O distances of these car-

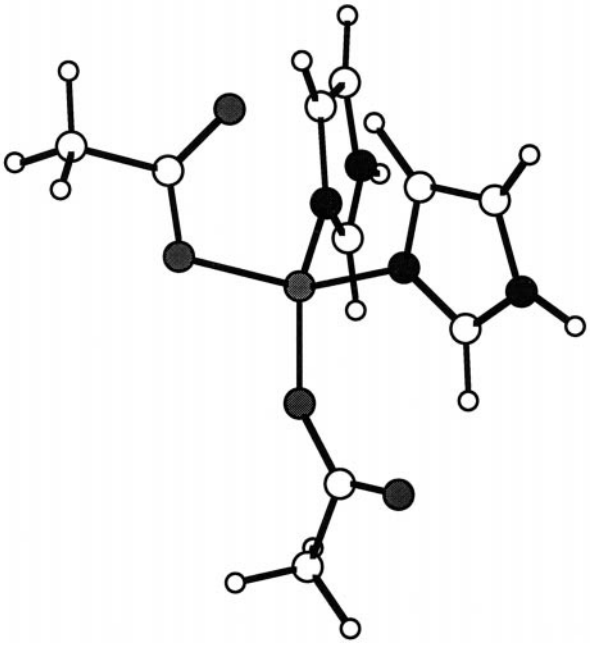

FIGURE 7 The optimized structure of $Zn(Im)_2(Ace)_2$.

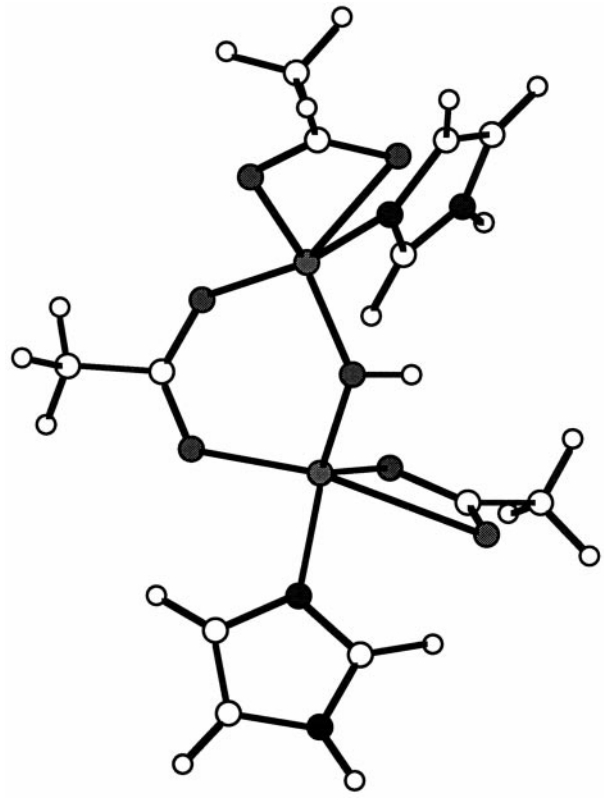

FIGURE 8 The optimized structure of (Im)(Ace)Zn(Ace)(OH)Zn-(Im)(Ace).

boxylate groups are 196/258 and 200/264 pm, which is quite similar to those observed in the crystal structures, although the longer distances are somewhat too long. As usual, the structure is stabilized by four hydrogen bonds from the imidazole CH groups to the carboxylate groups, two to the carboxylate oxygen with the longer Zn-O distance (226–244 pm), and two weaker to the bridging carboxylate group (271–310 pm).

We have also tried to optimize the corresponding complex with a bridging water molecule instead of the hydroxide ion. However, during the geometry optimization, a hydrogen of the water molecule moved to one of the carboxylate groups, leading to appreciable changes in the structure. Thus we must conclude that the bridging molecule is a hydroxide ion, and that bidentate neutral carboxylate-zinc complexes are possible also in vacuum, at least for bridged binuclear complexes.

Finally, we optimized the structure of $Zn(Im)_3(Ace)^+$. We selected this structure because we expected to see a smaller influence on the carboxylate coordination from the other ligands, inasmuch as the imidazole groups only provide CH groups as hydrogen-bond donors. The optimized structure of this complex is shown in Fig. 9 and described in Table 2. It is symmetrical, with two similar Zn-N bonds and one slightly longer Zn-N bond (204 and 208 pm). The coordination of the carboxylate group is intermediate between bi- and monodentate, with significantly different Zn-O bond lengths, 199 and 248 pm. The reason for this asymmetry is differences in the hydrogen-bond interactions of the two oxygens. The one with the shorter zinc bond forms a weak hydrogen bond (247 pm) with a CH group on the imidazole with the longer zinc bond. The other carboxylate group forms two stronger hydrogen bonds with CH groups on the other two imidazole rings (235 pm).

Interestingly, this is the only stable structure for this complex; there is no local minimum for a strictly bidentate structure or for a monodentate structure. Yet if the Zn-O-C angle is constrained to 120°, we could optimize a monodentate structure that is only 4 kJ/mol less stable than the optimal structure. This is in accord with available crystal structures; L-fuculose 1-phosphate aldolase, fructose 1,6-biphosphate aldolase, and reduced Cu,Zn-superoxide dismutase all have a $Zn(His)_3Glu$ coordination sphere for which $Zn(Im)_3(Ace)^+$ should be an adequate model. Interestingly, the first protein shows a bidentate carboxylate group, whereas the other two proteins have monodentate carboxylate groups (Lipscomb and Sträter, 1996). Similarly, a strictly bidentate structure, obtained with the Zn-O-C angle constrained to 90°, is also 4 kJ/mol less stable than the optimal structure.

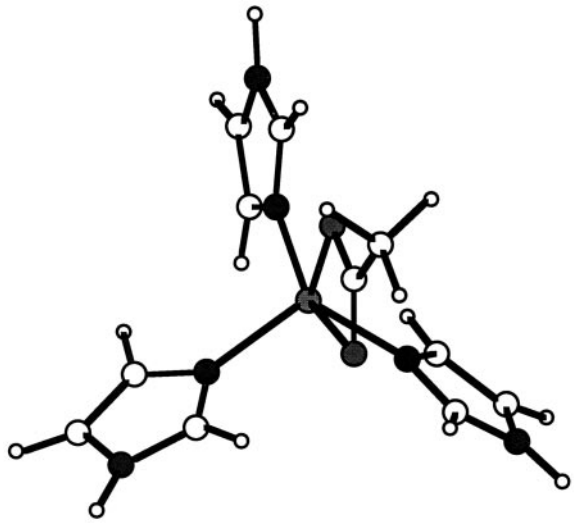

FIGURE 9 The optimized structure of $Zn(Im)_3(Ace)$.

Syn and *anti* coordination modes

A monodentate carboxylate group can coordinate to a zinc ion in two different ways, depending on the Zn-O-C-O dihedral angle. If this angle is around 0°, the coordination mode is called *syn* (*Z*-form; Zn and the noncoordination carboxylate oxygen are on the same side of the C-O bond). On the other hand, if the angle is close to 180°, the coordination mode is called *anti* (*E*-form), which normally gives weaker bonds. All complexes studied up to now have been in the *syn* coordination mode.

The relative stabilities of the *syn* and *anti* forms of carboxylic acids and carboxylic esters have been thoroughly studied by theoretical methods. For example, it has been shown that the *syn* form of acetic acid is more stable than the *anti* form by ~20–25 kJ/mol (22 kJ/mol with our methods) in gas phase, a value that is reduced to 4–8 kJ/mol if solvation effects are considered (Peterson and Csizmadia, 1979; Wiberg and Ladig, 1987; Chen et al., 1994; Nagy et al., 1994; Andzelm et al., 1995). It has also been noted that the *syn* form exhibits a higher basicity (~20 kJ/mol) and is therefore more effective for general-base catalysis (Gandour, 1981; Li and Houk, 1989). Nevertheless, there is only a small difference in the hydrogen-bond strength of the two conformations. For example, Li and Houk (1989) find only a 1-kJ/mol difference in the hydrogen-bond strength of the *syn* and *anti* forms of the $H_2NH\cdots OOCH$ complex. Similarly, we have calculated a *syn-anti* energy difference of the methanol-acetate complex of only 2 kJ/mol.

We have tried to optimize *anti* structures for all of the models in this investigation. The optimized structure of $Zn(Im)_2(Ace)(H_2O)^+$ is shown in Fig. 10. It is stabilized by two weak hydrogen bonds to the coordinating carboxylate atom, one from water and one from imidazole (208 and 284 pm). In addition, there is a weak hydrogen bond from imidazole to the water molecule (280 pm), but there is no interaction at all with the noncoordination carboxylate atom. Quite unexpectedly, we have not been able to find any local minimum for the *anti* coordination mode of $Zn(Im)_3(Ace)$ or $Zn(Im)_2(Ace)_2$. Both complexes reorganized to the optimal structures described above.

The energy differences between the *syn* and *anti* conformations of the various complexes are listed in Table 2.

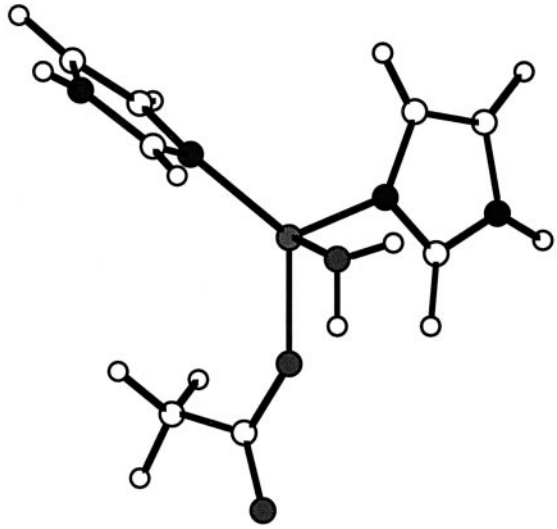

FIGURE 10 The optimized monodentate structure of $Zn(Im)_2(Ace)(H_2O)^+$ in the *anti* coordination mode.

Apparently, these energies are larger than for the hydrogen bonds. For the one-coordinate zinc-acetate complex, the difference is as high as 131 kJ/mol, but the energy is reduced to 97 kJ/mol in the three-coordinate $Zn(Im)_2(Ace)^+$ complex. In the $Zn(Im)_2(Ace)(H_2O)^+$ and $Zn(Im)_2(Ace)(OH)$ complexes the *syn/anti* difference is 88 and 68 kJ/mol, respectively. This is a large energy, but it is not insurmountable, considering that the energy of a hydrogen bond between a free acetate molecule and water is ~80 kJ/mol (due to the charge on acetate). This is in accord with the observation that all carboxylate groups coordinating to zinc in an *anti* mode in available crystal structures have hydrogen bonds to the uncoordinated oxygen atom (Chakrabarti, 1990). About 20% of the zinc-carboxylate complexes in the Cambridge Structural Database are in the *anti* conformation (Carrell et al., 1988).

CONCLUSIONS

By collecting the data of all of our optimized structures, a detailed picture of the Zn-carboxylate interaction starts to emerge. It can be summarized in the following way.

1. The carboxylate group itself is quite indifferent to its coordination mode, i.e., the potential energy surface is extremely flat (the force constant of the more weakly bound carboxylate atom is typically ~5 J/mol/pm^2, almost 10 times weaker than for the other ligands). Therefore, the coordination mode is determined mainly by other interactions within the complex. Moreover, the energy barrier between the various coordination modes is small (~6 kJ/mol).

2. In complexes with three or fewer zinc ligands, a bidentate coordination is preferred (by ~50 kJ/mol; see Table 2).

3. In complexes with four zinc ligands and a total charge of +1, bidentate and monodentate coordinations are inherently of about the same stability. Therefore, the coordination mode is determined mainly by possible hydrogen bonds to the carboxyl groups. In the $Zn(Im)_2(Ace)(H_2O)^+$ complex, a strong hydrogen bond stabilizes a monodentate coordination. In $Zn(Im)_3(Ace)^+$, the hydrogen bonds are much weaker, and a 1.5 coordination is the most stable state (Zn-O distances: 199 and 248 pm). Finally, in the strictly bidentate $Zn(Im)_2(Ace)(H_2O)^+$ complex (with almost the same binding energy as the monodentate complex), the hydrogen bonds are still weaker. Together this indicates that in the absence of hydrogen-bond interactions, the bidentate coordination mode is also probably more favorable for the positively charged four-coordinate zinc complexes. This is confirmed by the $Zn(Im)_2(Ace)(H_2O)^+$ complexes with one or two second-sphere water molecules.

4. In complexes with four zinc ligands and a total charge of 0, monodentate coordination is inherently more stable. Yet bidentate binding modes, and especially various intermediate coordinations, can easily be reached at a small energy expense, 5–22 kJ/mol. A hydroxide ion destabilizes bidentate complexes more than a carboxylate group.

5. In binuclear zinc complexes with bridging ligands, bidentate structures are also stable for neutral models in vacuum.

6. *Anti* coordination of carboxylate groups is much less stable than *syn* coordination, typically by 70–120 kJ/mol.

Altogether, this explains why both bidentate and monodentate structures are common among zinc proteins (~30% of the Zn-carboxylate proteins are bidentate (Alberts et al., 1998), whereas among smaller zinc complexes, ~10% are bidentate (Carrell et al., 1988)). It also shows that enzymes have the opportunity to modulate the coordination number of carboxylate-metal sites at almost no cost, which probably is of great importance in several zinc and iron proteins. On the other hand, this shallow potential makes the theoretical treatment of such sites hard, because the geometries converge slowly and there are several local minima with almost the same energy. Therefore there is a great risk of ending up in erroneous structures unless tight convergence criteria are used, as in the present investigation.

This investigation has been supported by grants from the Swedish Natural Science Research Council (NFR). It has also been supported by computer resources of the Swedish Council for Planning and Coordination of Research (FRN), Parallelldatorcentrum (PDC), at the Royal Institute of Technology, Stockholm, and the National Supercomputer Centre (NSC) at the University of Linköping.

REFERENCES

Ahlrichs, R., M. Bär, M. Häser, H. Horn, and C. Kölmel. 1989. Electronic structure calculations on workstation computers: the program system Turbomole. *Chem. Phys. Lett.* 162:165–169.

Alberts, I. L., K. Nadassy, and S. J. Wodak. 1998. Analysis of zinc binding sites in protein crystal structures. *Protein Sci.* 7:1700–1716.

Andzelm, J., C. Kölmel, and A. Klamt. 1995. Incorporation of solvent effects into density functional calculations of molecular energies and geometries. *J. Chem. Phys.* 103:9312–9320.

Bauschlicher, C. W. 1995. A comparison of the accuracy of different functionals. *Chem. Phys. Lett.* 246:40–44.

Carrell, C. J., H. L. Carrell, J. Erlebacher, and J. P. Glusker. 1988. Structural aspects of metal ion-carboxylate interactions. *J. Am. Chem. Soc.* 110:8651–8656.

Chakrabarti, P. 1990. Interaction of metal ions with carboxylic and carboxamide groups in protein structures. *Protein Eng.* 4:49–56.

Chen, J. L., L. Noodleman, D. A. Case, and D. Bashford. 1994. Incorporating solvation effects into density functional electronic structure calculations. *J. Phys. Chem.* 98:11059–11068.

Chevrier, B., C. Schalk, H. d'Orchymont, J. M. Rondeau, D. Moras, and C. Tarnus. 1994. Crystal structure of *Aeromonas proteolytica* aminopeptidase: a prototypical member of the co-catalytic zinc enzyme family. *Structure.* 2:283–291.

Christianson, D. W. 1991. Structural biology of zinc. *Adv. Protein Chem.* 42:281–355.

Christianson, D. W., and W. N. Lipscomb. 1989. Carboxypeptidase A. *Acc. Chem. Res.* 22:62–69.

De Kerpel, J. O. A., and U. Ryde. 1999. Protein strain in blue copper proteins studied by free energy perturbations. *Proteins Struct. Funct. Genet.* 36:157–174.

Dreyer, M. K., and G. E. Schulz. 1996. Refined high-resolution structure of the metal-ion dependent L-fuculose-1-phosphate aldolase (class II) from *Escherichia coli*. *Acta Crystallogr.* D52:1082–1091.

Dunning, T. H., and P. J. Hay. 1977. *In* Methods of Electronic Structure Theory, Vol. 2. H. F. Schaeffer, editor. Plenum Press, New York. 1–13.

Frisch, M. J., G. W. Trucks, H. B. Schlegel, G. E. Scuseria, M. A. Robb, J. R. Cheeseman, V. G. Zakrzewski, J. A. Montgomery, R. E. Stratmann, J. C. Burant, S. Dapprich, J. M. Millam, A. D. Daniels, K. N. Knudin, M. C. Strain, O. Farkas, J. Tomasi, V. Barone, M. Cossi, R. Cammi, B. Mennucci, C. Pomelli, C. Adamo, S. Clifford, J. Ochterski, G. A. Petersson, P. Y. Ayala, Q. Cui, K. Morokuma, D. K. Malick, A. D. Rabuck, K. Raghavachari, J. B. Foresman, J. Cioslowski, J. V. Ortiz, B. B. Stefanov, G. Liu, A. Liashenko, P. Piskorz, I. Komaromi, R. Gomperts, R. L. Martin, D. J. Fox, T. Keith, M. A. Al-Laham, C. Y. Peng, A. Nanayakkara, C. Gonzalez, M. Challacombe, P. M. W. Gill, B. G. Johnson, W. Chen, M. W. Wong, J. L. Andres, M. Head-Gordon, E. S. Replogle, and J. A. Pople. 1998. Gaussian 98, Revision A.5. Gaussian, Inc., Pittsburgh PA.

Gandour, R. D. 1981. On the importance of orientation in general base catalysis by carboxylate. *Bioorg. Chem.* 10:169–176.

Hall, T. M. T., J. A. Porter, P. A. Bechy, and D. J. Leahy. 1995. A potential catalytic site revealed by the 1.7-Å crystal structure of the amino-terminal signalling domain of Sonic hedgehog. *Nature.* 378:212–216.

Here, W. J., L. Radom, P. v. R. Scheyer, and J. A. Pople. 1986. Ab Initio Molecular Orbital Theory. Wiley-Interscience, New York.

Hertwig, R. H., and W. Koch. 1997. On the parameterization of the local correlation functional. What is Becke-3-LYP? *Chem. Phys. Lett.* 268: 345–351.

Holland, D. R., A. C. Hausrath, D. Juers, and B. W. Matthews. 1995. Structural analysis of zinc substitutions in the active site of thermolysin. *Protein Sci.* 4:1955–1965.

Holland, D. R., D. E. Tronrud, H. W. Pley, K. M. Flaherty, W. Stark, J. N. Jansonius, D. B. Mckay, and B. W. Matthews. 1992. Structural comparison suggests that thermolysin and related neutral proteases undergo hinge-bending motion during catalysis. *Biochemistry.* 31:11310–11316.

Holm, R. H., P. Kennepohl, and E. I. Solomon. 1996. Structural and functional aspects of metal sites in biology. *Chem. Rev.* 96:2239–2314.

Holthausen, M. C., M. Mohr, and W. Koch. 1995. The performance of density functional/Hartree-Fock hybrid methods: the binding in cationic first-row transition metal methylene complexes. *Chem. Phys. Lett.* 240: 245–252.

Li, Y. S., and K. N. Houk. 1989. Theoretical assessments of the basicity, and nucleophilicity of carboxylate syn and anti lone pairs. *J. Am. Chem. Soc.* 111:4505–4507.

Lippard, S. J., and J. M. Berg. 1994. Carboxypeptidase A and thermolysin: structral studies. Principles of Bioinorganic Chemistry. University Science Books, Mill Valley, CA. 259–262.

Lipscomb, W. N., and N. Sträter. 1996. Recent advances in zinc enzymology. *Chem. Rev.* 96:2375–2433.

Mangani, S., P. Carloni, and P. Orioli. 1992. Crystal structure of the complex between carboxypeptidase A and the biproduct analog inhibitor L-benzylsuccinate at 2.0 Å resolution. *J. Mol. Biol.* 223:573–578.

Matthews, B. W. 1988. Structural basis of the action of thermolysin and related zinc peptidases. *Acc. Chem. Res.* 21:333–340.

Matthews, B. W., J. N. Jansonius, P. M. Colman, B. P. Schoenborn, and D. Dupourque. 1972. Three-dimensional structure of thermolysin. *Nature New Biol.* 238:37–41.

Monzingo, A. F., and B. W. Matthews. 1984. Binding of *N*-carboxymethyl dipeptide inhibitors to thermolysin determined by x-ray crystallography: a novel class of transition-state analogues for zinc peptidases. *Biochemistry.* 23:5724–5729.

Nagy, P. I., D. A. Smith, G. Alagona, and C. Ghio. 1994. Ab initio studies of free and monohydrated carboxylic acids in the gas phase. *J. Phys. Chem.* 98:486–493.

Peterson, M. R., and I. G. Csizmadia. 1979. Determination and analysis of the formic acid conformational hypersurface. *J. Am. Chem. Soc.* 101: 1076–1079.

Rauhut, G., and P. Pulay. 1995. Transferable scaling factors for density functional derived vibrational force fields. *J. Phys. Chem.* 99: 3093–3100.

Rees, D. C., M. Lewis, and W. N. Lipscomb. 1983. Refined crystal structure of carboxypeptidase A at 1.54 Å resolution. *J. Mol. Biol.* 168:367–387.

Ricca, A., and C. W. Bauschlicher. 1995. A comparison of density functional theory with ab initio approaches for systems involving first transition row metals. *Theor. Chim. Acta.* 92:123–131.

Schäfer, A., H. Horn, and R. Ahlrichs. 1992. Fully optimized contracted Gaussian basis sets for atoms Li to Kr. *J. Chem. Phys.* 97:2571–2577.

Seminario, J. M. 1996. Calculation of intramolecular force fields from second-derivative tensors. *Int. J. Quant. Chem. Quant. Chem. Symp.* 30:59–65.

Shoham, G., D. C. Rees, and W. N. Lipscomb. 1984. Effects of pH on the structure and function of carboxypeptidase A: crystallographic studies. *Proc. Natl. Acad. Sci. USA.* 81:7767–7771.

Thayer, M. M., K. M. Flaherty, and D. B. Mckay. 1991. Three-dimensional structure of the elastase of *Pseudomonas aeruginosa* at 1.5-Å resolution. *J. Biol. Chem.* 266:2864–2871.

Vosko, S. H., L. Wilk, and M. Nusair. 1980. Accurate spin-dependent electron liquid correlation energies for local spin density calculations: a critical analysis. *Can. J. Phys.* 58:1200–1207.

Wang, Z., and F. A. Quiocho. 1998. Complexes of adenosine deaminase with two potent inhibitors: x-ray structres in four independent molecules at pH of maximum activity. *Biochemistry.* 37:8314–8324.

Wiberg, K. B., and K. E. Ladig. 1987. Barriers to rotation adjacent to double bonds. 3. The C-O barrier in formic acid, methyl formate, acetic acid, and methyl acetate. The origin of ester and amide "resonance." *J. Am. Chem. Soc.* 109:5935–5943.

Zhang, K., B. Chance, D. S. Auld, S. L. Larsen, and B. L. Vallee. 1992. X-ray absorption fine structure study of the active site of zinc and cobalt carboxypeptidase A in their solution and crystalline forms. *Biochemistry.* 31:1159–1168.